Synergistic Exploitation of Geoinformation Methods for Post-earthquake 3D Mapping and Damage Assessment

Nikolaos Soulakellis, Georgios Tataris, Ermioni-Eirini Papadopoulou, Stamatis Chatzistamatis, Christos Vasilakos, Dimitris Kavroudakis, Olga Roussou and Apostolos Papakonstantinou

Abstract This paper presents a methodological framework, which establishes links among the: i. 3D mapping, ii. 3D model creation and iii. damage classification grades of masonry buildings by European Macroseismic Scale-98 and the application of geoinformation methods towards 3D mapping and damage assessment after a catastrophic earthquake event. We explore the synergistic exploitation of a Real Time Kinematics system, terrestrial photogrammetry, Unmanned Aircraft Systems and terrestrial laser scanner for collecting accurate and high-resolution geospatial information. The proposed workflow was applied at the catastrophic earthquake of June 12th, 2017 on the traditional settlement of Vrisa on the island of Lesvos, Greece. The Structure from Motion method has been applied on the

N. Soulakellis (✉) · G. Tataris · E.-E. Papadopoulou · C. Vasilakos · D. Kavroudakis · O. Roussou · A. Papakonstantinou
Department of Geography, University of the Aegean, Mytilene, Greece
e-mail: nsoul@aegean.gr

G. Tataris
e-mail: tataris@geo.aegean.gr

E.-E. Papadopoulou
e-mail: geom17022@geao.aegean.gr

C. Vasilakos
e-mail: chvas@aegean.gr

D. Kavroudakis
e-mail: dimitrisk@aegean.gr

O. Roussou
e-mail: orousou@aegean.gr

A. Papakonstantinou
e-mail: apapak@geo.aegean.gr

S. Chatzistamatis
Department of Cultural Technology and Communication, University of the Aegean, Mytilene, Greece
e-mail: stami@aegean.gr

O. Altan et al. (eds.), *Intelligent Systems for Crisis Management*,
Lecture Notes in Geoinformation and Cartography,
https://doi.org/10.1007/978-3-030-05330-7_1

high-resolution terrestrial and aerial photographs, for producing accurate and very detailed 3D point clouds of the damaged buildings of the Vrisa settlement. Additionally, two Orthophoto maps and two Digital Surface Models have been created, with a spatial resolution of 5 cm and 3 cm, respectively. The first orthophoto map has been created just one day after the earthquake, while the second one, a month later. The significant advantages of the proposed methodology are: (a) the production of reliable and accurate 2D and 3D information at both village and building scales, (b) the ability to support scientists during building damage assessment phase and (c) the proposed damage documentation provides all the appropriate information which can augment all experts and stakeholders, national and local organizations focusing on the post-earthquake management and reconstruction processes of the Vrisa traditional village.

1 Introduction

Natural hazards such as earthquakes have an enormous effect on populated places regarding both life-threating conditions and socio-economic impact. An earthquake is a very crucial case of natural hazards, having the following characteristics: (a) it cannot be predicted; (b) only few seconds of a strong shake can cause enormous damage in large areas; (c) it can affect all aspects of society; (d) its effects can last for many years; and (e) the correct management of an earthquake risk relies on close cooperation between different organizations at different levels.

The response phase of an earthquake regarding emergency management is extremely complicated as: (a) the buildings are highly vulnerable to aftershocks; (b) many streets are not accessible; (c) seismic activity continues to produce several strong aftershocks affecting more the most damaged buildings; (d) relief operations are in action by several organizations; and (e) most people are frightened and some in panic. The planning and the implementation of the response in a natural disaster is mainly based on the precise information provided by the assessment. Post-disaster assessment can be done in four levels: (a) rapid assessment, (b) short-term recovery and (c) long-term reconstruction and (d) recovery management.

After an earthquake, remote sensing has been widely used in rapid damage assessment to detect either region with collapsed buildings or individual damaged buildings (Olsen et al. 2013; Dong and Shan 2013). In recent decades, airborne platforms and especially Unmanned Aerial Systems (UAS) have been utilized after earthquakes and each event presented different opportunities and lessons confirming UAS's usage for imagery collection, detection and damage estimation in disaster risk and emergency management (Adams and Friedland 2011; Gomez and Purdie 2016). In Dominici et al. (2017) the authors mention that recent technological advantages make UAS-based photogrammetry highly suitable for surveys in a geo-hazard context, as in a post-earthquake scenario, and its advantages may be summarized as follows: (i) safety: no risk for operators; (ii) possibility to survey

inaccessible zones; (iii) high-resolution photographs; (iv) speed of survey and elaboration; and (v) repeatability and economic convenience. More recently, UAS data where used for automatic extraction of buildings and their facades implementing segmentation on point clouds (Chen et al. 2016; Calantropio et al. 2018). Aerial surveys are often carried out using multiple small or medium-format cameras mounted together that simultaneously capture nadir and oblique images. Oblique images capture the scene under a tilt angle, having much larger footprint than in nadir views. The tilted cameras are improving the visibility of buildings facades and other vertical structures. These non-oblique camera views have as a result scale and visibility related errors due to their scale variations (Papakonstantinou et al. 2018).

Due to the very late advances in the fields of computer vision and photogrammetry in combination with the ever-increasing data processing power, orthophoto maps and Digital Surface Models (DSM) can be produced, by terrestrial and/or aerial high-resolution 2D imagery taken after an earthquake. The Structure from Motion (SfM) algorithm has improved the quality of 3D data that can be derived from overlapping imagery by incorporating advancements in soft-copy triangulation and image-based terrain extraction algorithms (Westoby et al. 2012; Bemis et al. 2014). Many studies have been carried out using UAS-SfM pipeline, emphasizing on near real-time data acquisition and processing after an earthquake event (Xu et al. 2014; Yamazaki et al. 2015; Papakonstantinou et al. 2018). In other cases, Object-Based Image Analysis (OBIA) applied to orthophoto maps to assess damage per building (Fernandez Galarreta et al. 2015).

Additionally, Terrestrial Photogrammetry (TP) and Terrestrial Laser Scanning (TLS) are efficient tools for post-earthquake damage assessment providing accurate high-resolution dense point clouds of areas of interest. TP and/or TLS can be used to collect precise 3D information of any object need to be estimated and reconstructed, such as debris, cracks in walls, non-structural damages, volume of individual buildings etc.

The application of TLS techniques for change detection and deformation monitoring of structures is an active area of research and many methods for that purpose have been already suggested (Chang et al. 2008; Zhihua et al. 2014; Mukupa et al. 2016; Guldur and Hajjar 2016; Erkal 2017; Guldur Erkal and Hajjar 2017; Jafari et al. 2017; Zhao et al. 2018; Puente et al. 2018). Olsen et al. (2013) utilize optical techniques, such as TLS and satellite imagery, to show that recently developed change detection algorithms can quickly provide regional damage information and they investigate damaged structures from the Indonesia and American Samoa tsunamis, San Diego coastal erosion, and cracking of a historical building in Italy. Anil et al. (2013) showed that it is possible to detect as small as $\sim$1 mm cracks from TLS data. They identified a series of crack parameters based on the state-of-the-art damage assessment codes and standards and parameters, which affect the performance of laser scanners for detecting cracks.

Many researchers focus on the application of TLS for the damage assessment after a disaster and research using TLS data has been conducted for damage assessment after several earthquakes. TLS data have been used for change detection of seismically-induced landslides from the 2004 Parkfield, California and 2004

Niigata Ken Chuetsu, Japan, Earthquakes (Kayen et al. 2006), and for various types of detailed measurements and analyses on structures from the 2010 Chile earthquake and tsunami, with data obtained in Concepción, Constitución, Dichato, and Talcahuano (Olsen et al. 2012).

The damage assessment and modeling with TLS data are presented for a four-story masonry-infilled reinforced concrete frame building, which was severely damaged due to the 2015 Gorkha Earthquake, Nepal (Bose et al. 2016) and for a two-story reinforced concrete masonry-infilled building which was severely damaged due to the 2010 El Mayor-Cucapah, Mexico earthquake (Song et al. 2018). Olsen and Kayen (2012) argue that the use of TLS can preserve the scene digitally for post-disaster assessment after the Japanese earthquake and tsunami. Application of TLS techniques is also found in (Pesci et al. 2013) where the authors propose a data analysis strategy with application to rapidly detect deformation traces in three buildings damaged by the 2012 Emilia Romagna earthquake in Italy.

Federal Emergency Management Agency's (FEMA) current state of Preliminary Damage Assessment (PDA) in local, state and federal scale includes structure-by-structure assessment by identifying damage facilities and documenting damage, work and cost. FEMA has established four categories to describe damage to homes; Destroyed, Major, Minor, and Affected with an Inaccessible category for the homes that cannot be reached for assessment. Geospatial Damage Assessment processes (GDAP) comprises self-reporting, fly-over surveying, door-to-door assessments, geospatial analysis and GIS, modeling and lately, integration of mobile technology (Federal Emergency Management Agency (FEMA) 2016).

The classification on the EMS-98 scale (European Macroseismic Scale) of damage is based on building types. Particularly, for each type of masonry structure, depending on the employed materials and construction techniques, an empiric vulnerability class is associated (descending scale from A to E) and the level of damage is categorized observing the structure (Grünthal 1998).

Even though geoinformation is rapidly expanding to several disciplines of both human and natural sciences, there is no robust methodology to apply in urgent situations such as after an earthquake for the creation of 3D models capturing its effects at a village scale. This paper focuses on a synergistic exploitation of latest geoinformation methods (TP, TLS, UAS) proposing a methodology for gathering precise and high-resolution 3D geoinformation (dense point clouds, 3D models of buildings or debris, DSM) where the building damage documentation can be modified in order to include all the 2D and 3D information produced.

This article describes the methodology followed the strong Lesvos 12 June 2017 (Mw = 6.3) earthquake which has heavily damaged the building stock of Vrisa traditional settlement covering an area of approximately 0.3 Km^2. The damages where widespread and about 80% of settlement's buildings were affected. Most of the buildings were traditional stone masonry residential constructions built by the end of the 19th century.

2 Methodology

The present methodological framework establishes links among the: i. 3D mapping, ii. 3D model creation and iii. damage classification grades of masonry buildings by EMS-98 which involves four stages: (a) data acquisition, (b) data processing, (c) data 3D modeling and 3D visualization and (d) visual damage assessment at two different scales: i. village-scale and ii. building-scale (Fig. 1). More analytically, data acquisition refers to: (a) Real Time Kinematics (RTK) measurements, (b) very high-resolution images acquired by UAS and terrestrial cameras and (c) point clouds acquired by terrestrial laser scanner.

RTK is a differential Global Navigation Satellite System (GNSS) technique which achieves positional measurements with accuracy in the range of a few centimeters, in the vicinity of a base station. This technique is based on the use of carrier measurements and the transmission of corrections from a base station with a known location, to the rover, so that the main errors that drive stand-alone positioning to cancel out. The RTK base station covers an area extending about 10 km, and a real-time communication channel is necessary for connecting the base and the rover.

Remote sensing offers several advantages in emergency situations, the first and foremost is the investigation and information acquisition in extremely hazard-prone zones. At first, for an 'early damage assessment', the high-resolution satellite images are very useful to detect quickly the areas and structures that suffered the worst damages. For a complete and very detailed survey of structures and infrastructures, useful for the following reconstruction phase, however, UAS photogrammetry is more suitable (Xu et al. 2014).

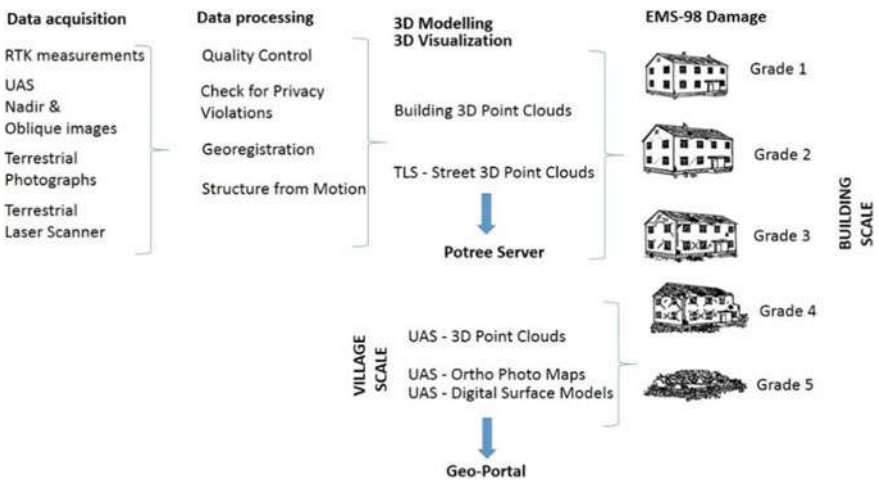

Fig. 1 Flowchart of the methodological framework for post-earthquake 3D mapping and building damage assessment of at two scales: i. village and ii. building

Photogrammetry is a cost-effective means of obtaining large-scale digital urban data. Photogrammetric techniques use 2D images without any prior data to create 3D data. Terrestrial, or ground-level, images are the most convenient data sources. Although these data provide high fidelity ground, vegetation, and building facade detail, they lack of building top information, and occlusion limits their range. The limited visible area in each image makes it difficult to construct large urban areas. In order to meet the specific goal of creating 3D models not only of the affected by the earthquake buildings (damaged) but of a whole building stock of a settlement, the photogrammetric survey planning should be based on the following criteria: i. optimize the number of the photos for each building, ii. maximize the accuracy of the information, iii. avoid privacy violations, iv. permit scale and registration of the 3D models and v. account for safety issues.

The Structure from Motion (SfM) algorithm, introduced in Computer Vision in the mid 90s, permits the automatic acquisition of the interior orientation parameters and the camera position in a relative image-space coordinate system. With SfM, scene geometry, camera position, interior and exterior orientation can all be extracted automatically, with high redundancy, using an iterative bundle adjustment (Triggs et al. 2000) on a sequence of images (multi-image approach). The principles and workflow of SfM have been described by (Snavely et al. 2008; Snavely 2011), and (Westoby et al. 2012). The Photoscan v1.3 software package was used for the SfM photogrammetric processing, which can convert many images into georeferenced DSMs, digital orthophotos and 3D models.

Terrestrial Laser Scanning has proven to be an increasingly practical technology for providing precise, accurate, timely and non-destructive estimates of human and natural objects in 3D models. Operational acquisition of TLS data, at a village scale, is possible due to the reduced instrument costs, the improved range, precision and accuracy of measurements, as well as the increased capability of software and computing infrastructure to process large datasets.

One of the main research concerns when using the above methods to acquire data is the assurance of protecting the privacy of the individuals since it is a common threat to include personal identity in this kind of data sets accidentally.

3 Application and Results

3.1 Study Area—Lesvos, June 12th, 2017 (m_w = 6.3) Earthquake

On 12 June 2017 (UTC 12:28:38.26) a magnitude Mw 6.3 earthquake occurred offshore the SE coast of Lesvos island in NE Aegean Sea, which was widely felt, caused one fatality, and partially ruined the village of Vrisa on the south-eastern coast of the island (Kiratzi 2018). Most of the traditional Vrisa buildings were damaged, several collapsed, while many were heavily damaged, reported dangerous

and/or unrepairable. Monument constructions, such as post-Byzantine churches suffered severe static effects. Fewer damages were widespread throughout the island (reported in at least 12 villages) (Papadimitriou et al. 2018).

Few days after the earthquake the Greek Earthquake Rehabilitation Organization (G-ERO) conducted first-degree inspections of the Vrisa buildings and most (not all) of the buildings were distinguished into the following three categories: i. "Green-Safe for Use", ii. "Yellow-Unsafe for Use" and iii. "Red-Dangerous for Use" according to the Earthquake Planning and Protection Organization guidelines. Typically, the last two categories, yellow and red, incorporate all degrees of damage according to the EMS-98 (Grünthal 1998), mainly from 3 (substantial-to-heavy) to 5 (destruction). Practically, the red category buildings should be demolished by their owners while the yellow category buildings could be reconstructed without being demolished.

The first-degree inspection results were marked with the appropriate signs on the buildings and mapped by means of a mobile geoinformation application. To conduct fast and collect geo-referenced data in the field, there was the need for a mobile application that could capture GPS coordinates along with some descriptive characteristics regarding the building structures of the village. For this purpose, a mobile application for Android Operating System (Nimodia and Deshmukh 2012) has been developed, that could capture the coordinates of the user along with a number of characteristics for each building. The application was based on the core code of OSMtracker application and was rebuilt with some extended functionality. The main panel of the mobile application includes button shortcuts for capturing house conditions (red cross, yellow cross, green cross). The shortcuts were used for rapid data collection in the field. Additionally, the following information of the buildings was collected: i. their geographical coordinates, ii. their constructed material (i.e., masonry R/C building) and iii. their number of stores (i.e., one, two or three floors) (Figs. 2 and 3) (see Table 1). Finally, the application includes voice notes collection, text notes collection and picture collection. All data are geo-referenced and can be processed with modern GIS systems.

3.2 Application

The synergistic exploitation of geo-information methods towards 3D mapping and damage assessment of the catastrophic earthquake of June 12th, 2017 on the traditional settlement of Vrisa on the island of Lesvos, Greece is presented in Fig. 4. One day after the earthquake a campaign started for collecting: (a) more than 150 ground control points using an RTK system, (b) more than 20.000 high-resolution terrestrial and aerial images using cameras and Unmanned Aircraft Systems and (c) 140 point clouds by a 3D Terrestrial Laser Scanner. The SfM method has been applied on the high-resolution terrestrial and aerial photographs, for producing

Fig. 2 Map presenting the distribution of first-degree inspections by the Greek ERO in combination with buildings' material

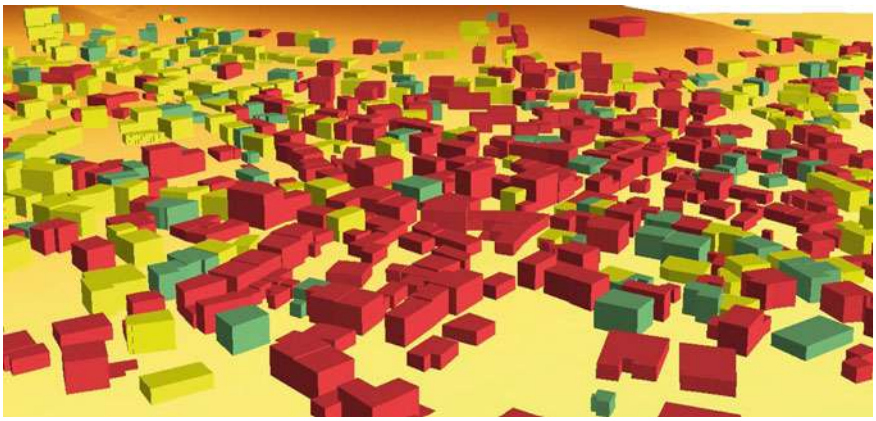

Fig. 3 3D visualization presenting the distribution of first-degree inspections by the Greek ERO in combination with buildings height. The buildings were distinguished into the following three categories: i. "Green—Safe for Use", ii. "Yellow—Unsafe for Use" and iii. "Red—Dangerous for Use" according to the Earthquake Planning and Protection Organization guidelines

Table 1 Information concerning the results after the first inspection by Greek ERO in accordance with building material and number of stories

	Number of buildings	Material			Number of Stories		
		Masonry	F/C	Mixed	1 Store	2 Store	3 Store
GREEN	218	165	46	7	125	91	2
YELLOW	314	310	8	6	122	186	6
RED	281	278	2	1	118	156	4
Uninspected	359						
Total	1162						

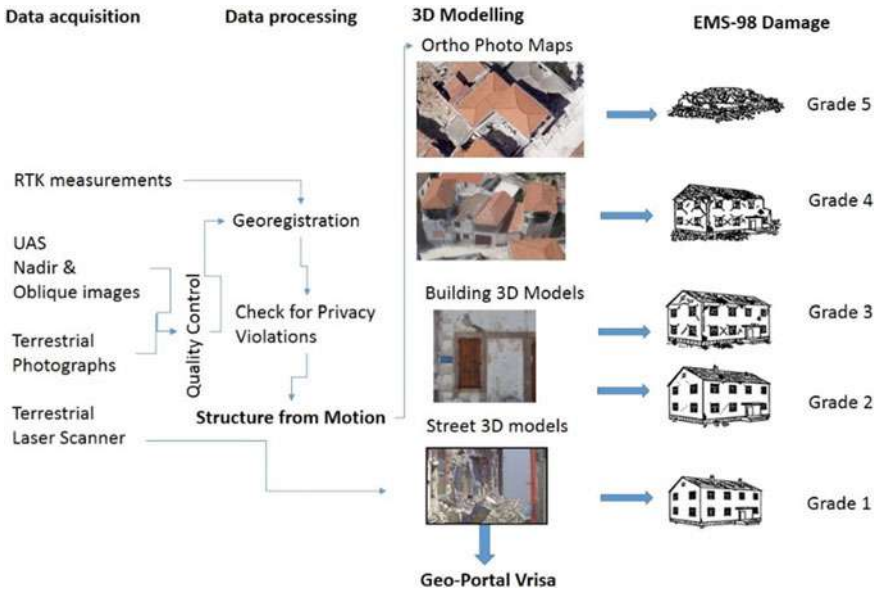

Fig. 4 Flow chart of the application of 3D mapping methods on Vrisa settlement after the catastrophic Lesvos earthquake

accurate and very detailed 3D point clouds of the damaged buildings of the Vrisa settlement. Additionally, two orthophoto maps and two DSMs have been created, with a spatial resolution of 5 cm and 3 cm, respectively.

The data acquisition campaign started on 13th June 2017, the very next day of the earthquake, under tough conditions and taking seriously into consideration the safety of the research team. During the following weeks, several very strong aftershocks occurred having magnitudes ranging from 3.5–5.0 Mw, producing more wall collapsing during the campaign.

During and following the data acquisition stage, quality control of all datasets was performed aiming to ensure the high quality of the results. Finally, the data processing and 3D modeling stages of the present methodology were carried out mainly by the application of the SfM algorithm.

3.2.1 Data Acquisition

The data acquisition stage involved several geoinformation data acquisition and processing methods and techniques: (a) RTK measurements, (b) high resolution aerial image collection by means of an UAS using an innovative multi-camera rig (Papakonstantinou et al. 2018), (c) high resolution photo collection by a DSLR camera, and (d) point clouds by a TLS and the relevant equipment.

RTK Measurements

The first important step of the campaign was the establishment of several Ground Control Points (GCPs) in Vrisa settlement with very high spatial accuracy and proper spatial distribution. These GCPs are necessary to enable georeferencing of all high-resolution aerial images as well as accurately identifying scan positions by the TLS. For this purpose, the following methodology was followed:

1. Two Base Stations (BS) were established within the village of Vrisa, depending on the base of the Greek National Trigonometric Network (NTN) located at the top of the hill named Korona, SW of the settlement of Vrisa. Due to the morphology of the settlement, as it is developed on three hills and two flat relatively low altitude surfaces, the two BSs were placed on the two hills on the outskirts of the settlement to be higher than the rest set of GCPs to achieve better and more accurate measurements.
2. One hundred fifty-seven (157) GCPs were placed within the Vrisa settlement, having very high accuracy in three dimensions (X, Y, Z), with an RTK rover, the base of which was placed at the one of the two base points, depending on the area where the GCPs were placed, to achieve better reception and a greater number of satellites, with an average horizontal error of 0.8 cm and an average elevation error of 1.3 cm. Thirty (30) of the GCPs, were used for georeferencing the orthophoto maps, resulting from the UAS images, having a suitable spatial distribution in the settlement.

UAS Nadir and Oblique High-Resolution Images

In less than 24 h after the strong earthquake, a UAS (hexacopter) flew over the Vrisa village at 160 m altitude and captured vertical images using a Sony A5100 camera with a fixed lens of 19 mm focal length. During the period 13/07/2017–6/

08/2017 several test flights was carried out with various aerial means and different sensors configuration to achieve a high-resolution mapping of the existing state of study area through the production of sub-decimeter spatial resolution orthophoto maps. The mapping of the Vrisa village was carried out with flights at different heights to explore the most efficient parameters of collecting data to record the damages of the area's buildings in an optimal way. Almost one and a half month later, on 25th July 2017, an innovative noncommercial multicamera rig attached to a UAS, flew a lower altitude (65 m), capturing high resolution images with: i. one nadir and ii. three (3) oblique cameras (angle $\theta = 45°$) having bottom, front and left-right configuration.

Terrestrial High-Resolution Images

During the period from 13th of June 2017 to 6th of July 2017, a survey for terrestrial high-resolution image acquisition took place using two Nikon D3400 cameras with 24.2 MP resolution, 23.5 × 15.6 mm sensor size and 6000 × 4000 pixel resolution, having the following standard settings: Aperture mode (f/8), Focal length: 18 mm, Production of raw JPEG images and Vibration Reduction disabled.

More specifically, the Vrisa settlement was divided into 240 road sections where each section included not more than five buildings and about 20,000 photos were taken covering all the buildings of Vrisa village, taking into serious consideration that the post-earthquake activity was in progress and many aftershocks with magnitude 4–5 were frequently occurring.

It is worth mentioning that photography on narrow-walled roads created a problem with the construction of a 3D model for tall buildings, because a large percentage of the facade was either not visible due to a balcony or was visibly tilted to the level of the camera. Note that with the specific cameras and settings the size of the visible field (field of view) at a distance of 3 m from a building is 3.92 m 2.6 m. This caused difficulty in matching images because in such a small range it was often difficult to locate uniquely distinct spots to identify in more than one photograph. The existence of a smooth pattern such as the wall without any features or rectangular rails creates a problem in identifying common features between consecutive photos. In some cases with no visible scale, measurements of distinct objects from the TLS data were used to scale the model.

Terrestrial Laser Scanning

The laser scan planning was designed with the aim of scanning not only the affected by the earthquake buildings (damaged) but the whole building stock of the Vrisa traditional settlement. Taking into consideration the TLS technical specifications and the Vrisa settlement characteristics, a network of one hundred forty scanner positions were established, that allowed maximum coverage of the settlement and guaranteed point spacing less than 1.5 cm for the whole settlement. The scan

planning was also based on the following criteria: i. optimization of the spatial distribution of the scans, ii. minimization of the number of the TLS scans, iii. minimization as possible of the occlusions, iv. avoid privacy violations (scan positions inside private property) and v. provide enough overlap (>30%) between consecutive laser scans, without using artificial targets.

Based on the criteria mentioned above, during the period from 13th June 2017 to 06th July 2017, a survey for TLS data acquisition performed by using a phase-shift laser scanner, FARO Focus^{3D}. One hundred forty (140) laser scans were performed from pre-measured positions using the RTK measurements. The scans were conducted with the following settings on the laser scanner: i. scan area: 360° horizontally × 305° vertically, ii. ¼ resolution that acquires point clouds at point spacing of 6.13 mm/10 m and thus less than 1.5 cm for the whole scenario of the settlement and iii. digital compass and inclinometer measurements.

The combination of the measured scanner position with the measurements from the compass and the inclinometer offers the option of a sensor-driven method for georeferencing the laser scanner data.

3.2.2 Data Processing

Quality Control and Check for Privacy Violations

After image acquisition, quality photo scans were followed to remove those that did not meet specific criteria, such as shifted scans as well as those in which there were objects in motion. Finally, the 3D Point Model acquired the texture of the buildings through the photos to create a photo-realistic object of the entire segment.

Visual inspection of all TLS data was performed in order to assess the quality of the point clouds. Scene software package by FARO was used for the TLS data processing. The raw point clouds were cleaned from noise or undesired information such as vegetation. In cases where errors were detected (due to dust on the scanner's rotating mirror and passing vehicles), the specific scans were reshaped. Also, dozens of control distances were taken to objects in the area for comparison with digital models. These distances were taken on fixed objects (windows, doors, etc.) with a tape measure. Next, the accuracy of the scalability of the point cloud resulting from scanning with the TLS and the extent to which these measurements correspond to the actual sizes of the measured objects was determined.

Finally, a detailed and systematic review of every element of the dataset was conducted for establishing and eliminating any form of violation of citizens' privacy through their direct or indirect identification from the data used. The examined data set included: i. ground images taken with a camera, ii. 3D models produced by TLS and by terrestrial photogrammetry, and iii. photos taken by UAS flights. The methods applied for the protection of citizens' privacy were the following: (a) Removal of citizens included in the data set, (b) blurring of the parts of the images and models in cases where the specific parts could not be removed.

Geo-Registration and Accuracy Assessment

Geo-registration is a crucial step in order to provide absolute orientation and to assign the proper scale to all derivatives of the spatial data acquisition process, such as the orthorectified aerial high-resolution images, the point clouds etc. Thus, it is necessary to add an adequate number of GCPs measured, in the Greek reference system GGRS-87, using the RTK technique. Subsequently, through the bundle adjustment, the GCPs together with the tie-points allow the internal and external orientation to be refined and directly obtain the geo-referenced model. Additionally, the geo-referenced 3D models must be verified using 'ground truth' measurements, several control points (CPs) to meet the purpose of providing reliable and verified metric quantification, as required in the case of the post-earthquake damage assessment.

On the UAS surveys 20 GCP's were used with a total RMS of 2.3 cm. The products generated for Vrisa village had geo-registration accuracies (RMS) less than a half of a pixel of the derivatives' resolution. From the geo-registration accuracy achieved can be concluded that the precision of the geoinformation produced is of satisfactory accuracy for post-earthquake damage assessment.

Regarding terrestrial photogrammetry, geo-rectification of each 3D model was performed upon request in order to visualize and analyze it with other georeferenced spatial data. The GCPs were collected from the orthophoto map derived from UAS data and the resulted accuracies were less than 10 cm.

3D Modeling with the SfM Method

The Photoscan v1.3 software package was used for the SfM photogrammetric processing, which can convert many images into georeferenced DSMs, digital orthophotos and 3D models. The datasets acquired for the specific post-earthquake situation were i. DSMs; ii. Orthophoto maps; and iii. 3D models. More specifically, the final products obtained by the methodology described above, were the following: i. Orthophoto map and DSM (13th June 2017), ii. Orthophoto map and DSM (25th July 2017), iii. Digital Elevation Model (DEM) of the Vrisa area having spatial resolution 5 cm and vertical accuracy less than 1 m, iv. 240 3D models of all the buildings of Vrisa settlement.

Geoportal and 3D Point Cloud Visualization

Within the context of this application, there was also a need for sound management and visualization of a large volume of spatial information. In addition, there existed a need to visualize their spatial distribution so that they could be asynchronously and remotely studied. For this purpose, it was considered necessary to design and implement an online geoportal which is hosted on a server, accessible only by authorized users. The design considered the needs of the application to monitor the

initial data, as well as the need for online visualization of the final data from each method. The technologies used to construct the geoportal consisted of several programming languages for the construction of data structures, by server-side technologies and by client-side technologies. The technologies used included the PHP and Python programming languages. The management of the complex geo-data structures in the embedded GeoServer and the database has been achieved by using Postgresql as it offers spatial data structures management capabilities.

Geocomputation projects such as the one conducted after the Vrisa Earthquake, asks for specialized handling of the results. The type and size of results as well as the sensitivity of information included, require a fast and reliable way of visualizing data and results. Relevant stakeholders such as local authorities and property owners, need to have customized access to specific parts of the project results. Therefore, a customized web application has been developed in the following URL: https://vrisa.aegean.gr mainly for results dissemination and data management. We used an open source WebGL-based point cloud renderer (Schütz 2016) in order to present results from 3D scanning process (Fig. 5). The web application was also used for centralized data management of intermediate results of the project and allowed for multi-platform access of the visualization. Finally, one of the main advantages of this web application was the concurrent multi-role access of users based on roles. Figure 6 depicts the main view of the web application which includes a separate panel on the left part, for the configuration of the visualization panel. One of the main advantages of this work is the ability to disseminate results to a variety of stakeholders that do not necessary share the very same knowledge and perspective of the scientific results and the results of the Vrisa Project. In other words, this web application bridges the gap between experts and public as well as the gap between technical and administrative individuals.

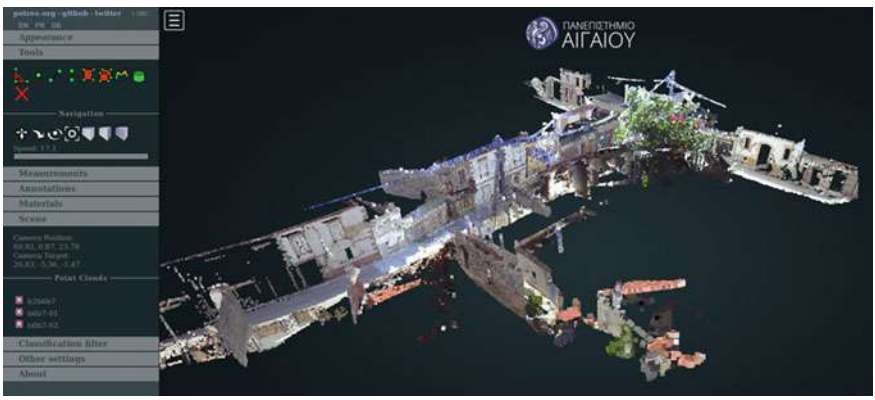

Fig. 5 Web-application (Potree) of the "Vrisa project" showing three interconnected 3D-scans in the main square of the village

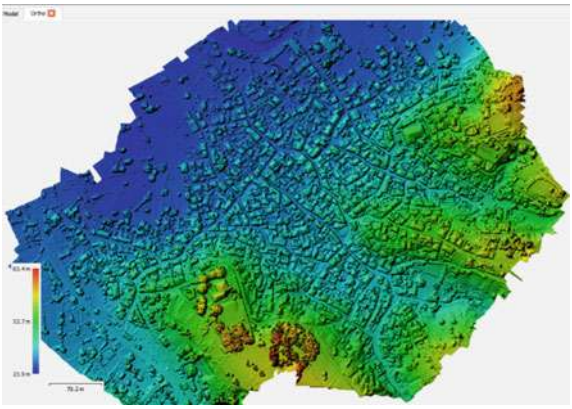

Fig. 6 Digital surface model map provided by the 13th June 2017 campaign, at a scale of 1:4.000 proved to be useful for the estimation of the collapsed and partially collapsed buildings

4 Discussion

4.1 Orthophoto Maps, Digital Surface Models and 3D Point Clouds by UAS Campaigns

4.1.1 UAS Campaign on June 13th, 2017

By processing the 229 nadir, high-resolution aerial images obtained the day after the earthquake, from an altitude of 160 m., an orthophoto map, a digital surface model (Fig. 7) and a 3D point cloud has been produced and proved to be very efficient in 'early damage assessment' stage. The results, required only a few hours of processing due to the small number of photos, capturing all the important information and providing a clear view of the heavily damaged areas of the Vrisa settlement, as well as those that were not essentially affected.

More analytically, the 13th June 2017 orthophoto map was visually interpreted aiming to produce an early severe-damage assessment map of the Vrisa settlement. Collapsed and partially collapsed buildings can be visually identified, showing clearly that heavy damages are concentrated on the western part of the village than on the eastern part. In parallel, blocked roads by heavily collapsed building as well as smaller debris by partial wall collapse can be clearly seen and mapped (Fig. 9). Based on the EMS-98 (Grünthal 1998) damage classification on the specific orthophoto map, damages of grade 5: destruction, e.g. partial and total collapse of buildings can be clearly visually identified giving an accurate early impact assessment in a short period of time (less than one day).

Fig. 7 3D Profile views of the 3D PointCloud (13/06/2017). Collapsed buildings can be clearly distinguished due to their smaller heights

Additionally, the DSM of Vrisa settlement (Fig. 6) derived by the processing of the 229 nadir UAS images provides a very effective mean to measure building heights after the earthquake, giving an estimation of their volume, and the possible extent of their total or partial collapse. Moreover, 3D visualization of the 3D point cloud gives the opportunity to visually explore the entirely collapsed buildings due to their smaller heights compared with the surrounding buildings (Fig. 7).

In addition, UAS high-resolution image acquisition, from medium altitudes i.e. 160 m, provides in a very short time a concise view of the earthquake affected areas. Furthermore, by visual interpretation very accurate and reliable information concerning the severity of an earthquake can be mapped, giving a very precise assessment for buildings having very heavy structural damages (grade 5), which can be taken into consideration for initiating effective emergency response and recovery actions (Fig. 8).

4.1.2 UAS Campaign on July 25th, 2017

The UAS data acquisition campaign that took place on July 25th, 2017, was implemented using an innovative Malteser cross configuration 4-camera rig. In this campaign, 1.044 nadir and 4.084 oblique high-resolution images (Fig. 9) were

Fig. 8 Orthophoto map of 13th June 2017 at a scale of 1:1.000 showing the NW part of Vrisa settlement which concentrates a large number of building of grade damages 5 e.g. partial and total collapse of buildings, the blocked roads and the areas with debris

Fig. 9 Part of a nadir (left) and oblique (right) image acquired on 25th June 2017. A serious failure of the top part of a wall is captured only on the oblique image (right)

Fig. 10 Parts of the 3D point cloud derived by nadir and oblique images acquired on 25th June 2017, where building damages of grade 4 are clearly identifable

Fig. 11 Orthophoto map of 25th June 2017 at a scale of 1:1.000 showing the NW part of Vrisa settlement which concentrates a large number of building with damages of grades 4 and 5

acquired, from an altitude of 65 m and processed with the SfM method. The derivatives were the sparse and dense 3D point clouds (Fig. 10), a DSM, a 3D model (mesh), and an orthophoto map (Fig. 11).

The produced orthophoto map, having a spatial resolution of 3 cm, presents clearly: i. totally or/and partially collapsed buildings, ii. roof damages (chimney collapse, roof detachment, etc.) and iii. debris close to the buildings that are reliable indicators of wall detachments and wall collapse. As such, visual interpretation of the orthophoto map can assist damage assessment especially for damages of grades 4 and 5.

More analytically building damages of grade 4: very heavy damage (heavy structural damage, very heavy non-structural damage: serious failure of walls; partial structural failure of roofs and floors) assessment requires reliable information from the building facades and not only from the roofs. For this reason, the 4.084 oblique high-resolution images from an altitude of 65 m enrich the data into the 3D models by providing more information from the building facades. Subsequently, visual interpretation of the building facades was made to identify the differences between the 3D models that were developed only from the nadir images and those from the combination of nadir and oblique accordingly (Fig. 10). As it was expected the 3D point cloud derived only from nadir images has a large number of gaps on the building's facades giving the wrong impression of extensive wall detachments and collapse. On the other hand, the 3D point cloud derived by processing both nadir and oblique images provide a more reliable 3D information, showing clearly the severe failure of building walls.

Based on the EMS-98 damage classification, on the specific orthophoto map and 3D point cloud, building damages of grade 4-very heavy damage (heavy structural damage, very heavy non-structural damage) serious failure of walls; partial structural failure of roofs and floors, can be visually identified. Building damages of grades 1, 2 and 3 are not identifiable. These results highlight the importance of applying suitable UAS configurations and flight planning characteristics, e.g. low altitude, more than one oblique cameras on board, to achieve more detailed and reliable 3D information (Fig. 10).

3D Point Clouds by TP and TLS

Several studies reveal that two main types of visual interpretation can be performed: i. the exploitation of the images for the detection of cracks or damages on the external surfaces of the building (i.e. walls and roofs) and ii. the use of point clouds (generated by photogrammetric approach) to detect structural anomalies such as tilted or deformed surfaces. In both cases, the automated processing can only support and ease the work of the expert, who still interprets and assesses the structural integrity of the building (earthquake damage).

Fig. 12 Part of a 3D model produced by terrestrial photogrammetry

Fig. 13 Measuring the deformation of wall from a TLS point cloud

All the 240 3D Point Clouds (Fig. 12) and the 140 Point Clouds of the 3D laser scanner (Fig. 13), created by TP and TLS respectively, provide the most important 3D information for assessing building damages of: i. grade 1: negligible to slight damages of the buildings, ii. grade 2: moderate damages, e.g. cracks in many walls, detachment of small pieces of places from the walls and partial collapse of chimneys, and iii. grade 3: substantial to heavy damages e.g. large and extensive cracking of all masonry load-bearing walls, detachment of large pieces of plaster in all load-bearing walls, dislocation and fall of roof tiles, detachment of the roof from the rest of the structure and fall of gables. Their very high resolution and accuracy permit the identification of hair-line cracks in walls, fall of small pieces of plaster only, falls of loose stones from upper parts of buildings and measure their characteristics (length and width of cracks, volumes of debris from falls, etc.).

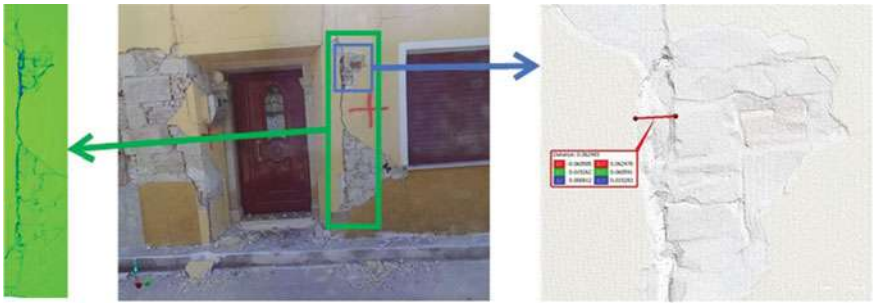

Fig. 14 Finding cracks on buildings and measuring in detail the dimension of cracks from a TLS point cloud

The ability to perform measurements is a very critical issue as post-earthquake situation is not suitable for that (Fig. 14). Especially during the first days after the disaster, it is impossible to get close enough to the buildings. Also, measurements on the upper parts of the buildings cannot be performed because it is impossible to access these parts of the buildings.

4.1.3 Building Damage Assessment Documentation

The EMS-98 presents several examples of building damage documentation, around the world, with a very comprehensive one-page document. This page provides few indicative photos, a general description of the site as well as information about the type of structure and the grade of damage of the building.

By the proposed methodology, the building damage documentation can be expanded to include all the 2D and 3D information produced and assist experts to visualize and measure building characteristics. The appropriate format is 3D-PDF because it is widely used, it permits the inclusion of 3D models and it offers: i. visualization tools (zoom-in, zoom-out, rotation etc.) and ii. a set of 2D and 3D measurement tools for measurements of lengths, areas, angles and volumes.

The proposed documentation includes four pages:

i. the first page presents all the important information concerning the building such as geographical position, type of structure, grade of damage and all the technical characteristic of the 3D point cloud produced by terrestrial photogrammetry (Fig. 15),
ii. the second page contains the 3D point cloud derived by terrestrial photogrammetry of the building, and with the 3D measurement tool it is possible to access the model and perform measurements of distances, angles and volumes (Fig. 16),

Geographical Position	Greece	DAMAGE ASSESSMENT
Coordinate System: **WGS-84** Longitude: 39.040362160982 Latitude: 26.200420640525 **TYPE OF STRUCTURE:** Masonry	**Lesvos earthquake Mw 6,3** **12/06/2017** **Lesvos island** **Village: Vrisa**	Grade of Damage (EMS-98): 1 | 2 | 3 | 4 | 5 — X Grade of Damage (ERO): Green | Yellow | Red — X

3D Model Technical Characteristics	
Number of Photos	19
Number of Points	20.157
Spatial Accuracy	0.004 (m)

Comment: The extensive broken walls suggest damage of grade-4.

Indicative Photo(s)

Fig. 15 An example from the first page of the proposed documentation of building damage assessment. It contains all the important information concerning the building such as: geographical coordinates, type of structure, grade of damage and all the technical characteristic of the 3D point cloud produced by terrestrial photogrammetry

Fig. 16 An example from the second page of the proposed documentation of building damage assessment which contains the 3D point cloud obtained by the high-resolution terrestrial photos. The 3D measuring tool permits the accurate measurement of distances, angles and volumes

Fig. 17 An example from the third page of the proposed documentation of building damage assessment, which contains the 3D point cloud derived by TLS. The 3D measuring tool permits the accurate measurement of distances, angles and volumes

iii. the third page contains the 3D point cloud derived by TLS, and with the 3D measurement tool it is possible to access the model and perform measurements of distances, angles and volumes (Fig. 17),

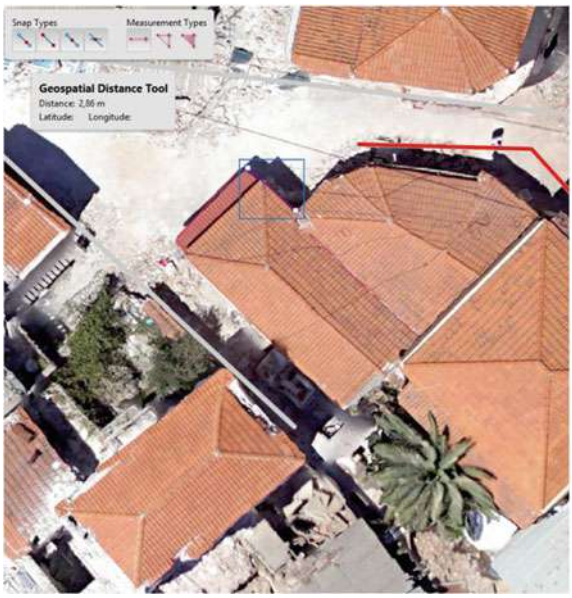

Fig. 18 An example from the fourth page of the proposed documentation of building damage assessment, which contains the part of the high resolution orthophoto map presenting the damaged building. The measuring tool permits the accurate measurement of distances and surfaces

iv. finally, the fourth page contains the appropriate part of the high resolution orthophoto map presenting the building and/or buildings, and with the 2D measurement tool it is possible to access the map and perform measurements of distances and areas (Fig. 18).

During the present study, a building damage assessment has been performed based on the results obtained by the followed methodology (Fig. 19). It is worthy to mention that the current damage assessment results should not be considered as fully reliable because all datasets involved cover only the external parts of the buildings. The damage evidence that can be captured from the orthophoto maps and 3D Point clouds could not consider sufficient to infer the actual damage state of the building as it requires damages to the internal building elements (e.g., columns and beams) that cannot be directly defined from the images and 3D point clouds. Despite the fact that this information is limited to the external part of the buildings, the images can provide useful information about the external condition of the masonry buildings, showing damages and providing a first important piece of information for structural engineers. Taking into consideration all the above, the results obtained by the damage assessment are summarized in Table 2.

The comparison between these results with the equivalent assessment derived by the Greek ERO shows that: i. the majority (70%) of the GREEN-buildings has been evaluated having damages of grade-1 while only 12% having damages of grade-2,

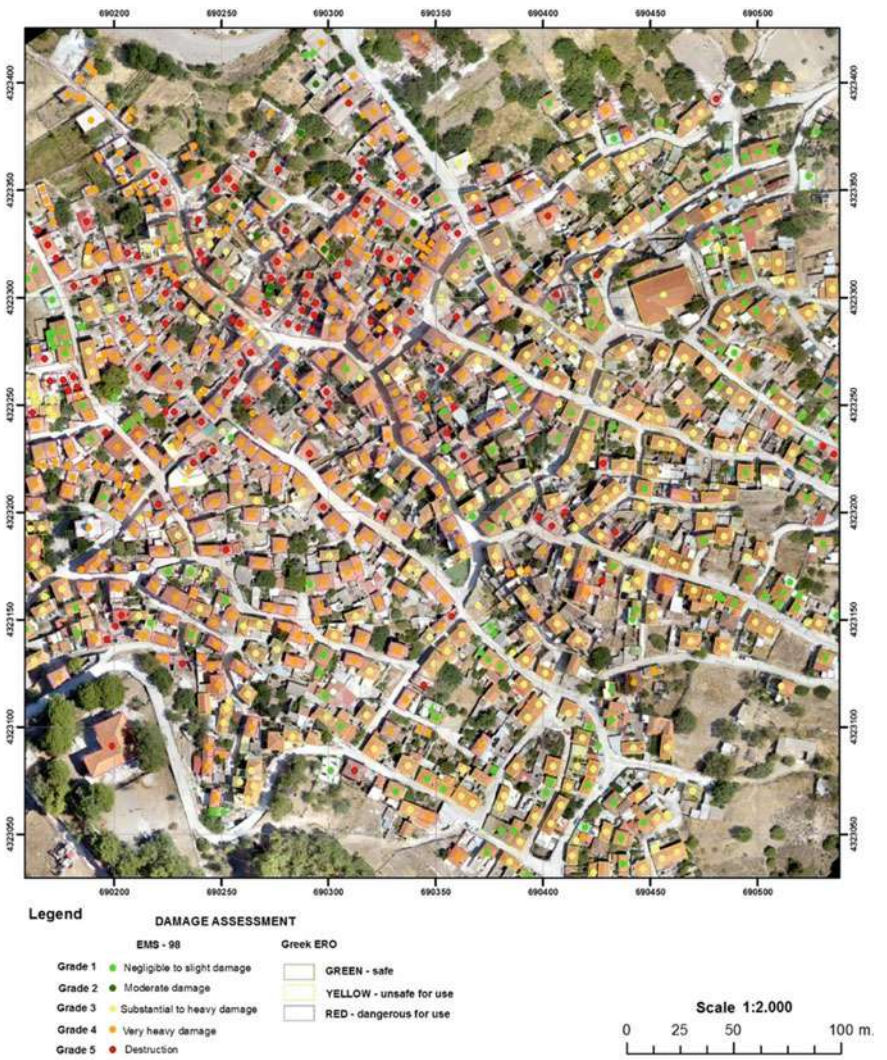

Fig. 19 Orthophoto map of 25th June 2017 at a scale of 1:2.000 presenting Vrisa settlement witch damage assessment results by: i. first inspection by Greek ERO and ii. by the use of the 3D Point Clouds produced during the present study

ii. the majority (78%) of the YELLOW-buildings has been evaluated having damages of grade-3 while only 10% of grade-4 and finally iii. the majority (64%) of the RED-buildings has been evaluated having damages of grade-4 and only 23% of grade-5 (see Table 3).

Table 2 Statistical information of the building damage assessment results obtained based on the visual interpretation and of the orthophoto maps and 3D Point clouds generated during the present study

	Number of buildings	Material			Number of Stories		
		Masonry	F/C	Mixed	1 Store	2 Store	3 Store
Grade 1	220	170	45	5	129	83	1
Grade 2	43	42	1	0	38	5	0
Grade 3	410	394	9	7	225	181	4
Grade 4	360	356	2	2	202	152	6
Grade 5	129	129	0	0	101	27	1
Total	1162						

Table 3 Comparison between damage assessment results, according to EMS-98 classification grades, based on the visual interpretation of the orthophoto maps and 3D Point clouds generated during the present study and the damage assessment results by the Greek ERO

Greek ERO	Number of buildings	EMS 98				
		Grade 1	Grade 2	Grade 3	Grade 4	Grade 5
GREEN	218	152	27	1	4	1
YELLOW	314	2	7	246	31	3
RED	281	1	3	8	179	64

5 Conclusions

The ambitious goal of the present study was to tackle all the difficulties of a post-earthquake scenario, in order to apply 3D mapping methodologies simultaneously to two different scales: i. village, and ii. building. Both scales are important in order to document the earthquake damages occurred to the Vrisa traditional settlement, by providing metrical information to permit building damage assessment according to the five (5) EMS-98 damage classification grades.

The fact that geoinformation, in a post-earthquake scenario, provides a great spectrum of methods, techniques and algorithms to calculate and measure 3D information, in two spatial scales, their synergistic application proved to be very promising for further research and development of semi or fully automatic methodologies.

More specifically: i. the orthophoto maps and DSMs derived by UAS flights in medium heights, e.g. 160 m., proved to be a very efficient mean for providing an early impact assessment at a village scale because it permits the accurate mapping of the totally or partially collapsed buildings, as well as blocked roads and debris, ii.

the 3D point cloud provided by the nadir and oblique high-resolution images acquired by UAS low altitude flight (65 m) proved to be suitable from mapping building damages of grade 4 as it illustrates efficient information concerning the building facades, iii. The 3D point clouds provided either by TP or by TLS proved to be the most accurate for mapping building damages of grades 3, 2 and 1 because they are evidencing anomalies and damages and providing a first important piece of information for structural engineers.

Finally, all 3D models would be useful for a post-earthquake management and reconstruction processes. Also, 3D mapping of an earthquake damaged traditional settlement is of great importance because after a short period most of the heavily damaged building will be demolished, destroying all their morphological characteristics, including their construction material and morphology of a traditional house. The proposed damage documentation provides all the appropriate information which can augment all experts and stakeholders, national and local organizations focusing on the post-earthquake management and reconstruction processes of the Vrisa traditional village.

Acknowledgements This paper is a result of the research project "3D mapping of Vrisa settlement after the 12th June Lesvos earthquake" funded by the North Aegean Region. The authors would like to thank Prof. Pavlogeorgatos G., Chaidas K., Kalaitzis P., Kaloniatis Ch., Doukari M., Drolias A., Mauroeidi A., Zorbas K., Papazis N., Moustakas, A. and Makri D. for supporting the processing stage of this project. In this publication the work related to UAS data acquisition and UAS-SfM process has been carried out within the framework of the Greek State Scholarship Foundation (I.K.Y.) Scholarship Programs funded by the "Strengthening Post-Doctoral Research" Act from the resources of the OP "Human Resources Development and Lifelong Learning "priority axis 6, 8, 9 and co-financed by the European Social Fund–ESF and the Greek government.

References

Adams SM, Friedland CJ (2011) A survey of unmanned aerial vehicle (UAV) usage for imagery collection in disaster research and management. In: Proceedings of the ninth international workshop on remote sensing for disaster response. Stanford, CA, USA, pp 15–16

Anil EB, Akinci B, Garrett JH, Kurc O (2013) Characterization of laser scanners for detecting cracks for post-earthquake damage inspection. In: 30th ISARC. Montreal, Canada, pp 313–320

Bemis SP, Micklethwaite S, Turner D, James MR, Akciz S, Thiele ST, Bangash HA (2014) Ground-based and UAV-Based photogrammetry: a multi-scale, high-resolution mapping tool for structural geology and paleoseismology. J Struct Geol 69:163–178. https://doi.org/10.1016/j.jsg.2014.10.007

Bose S, Nozari A, Mohammadi ME, Stavridis A, Babak M, Wood R, Gillins D, Barbosa A (2016) Structural assessment of a school building in Sankhu, Nepal damaged due to torsional response during the 2015 Gorkha earthquake. In: Pakzad S, Juan C (eds) Conference proceedings of the society for experimental mechanics series, Dynamics of civil structures. Springer, Cham, pp 31–41

Calantropio A, Chiabrando F, Sammartano G, Spanò A, Losè LT (2018) UAV strategies validation and remote sensing data for damage assessment in post-disaster scenarios. Int Arch Photogramm Remote Sens Spat Inf Sci XLII-3/W4:121–128. https://doi.org/10.5194/isprs-archives-xlii-3-w4-121-2018

Chang KT, Wang EH, Chang YM, Cheng HK (2008) Post-disaster structural evaluation using a terrestrial laser scanner. Integrating generations FIG working week 2008. Stockholm, Sweden, pp 1–15

Chen J, Liu H, Zheng J, Lv M, Yan B, Hu X, Gao Y (2016) Damage degree evaluation of earthquake area using UAV aerial image. Int J Aerosp Eng 2016:1–10. https://doi.org/10.1155/2016/2052603

Dominici D, Alicandro M, Massimi V (2017) UAV photogrammetry in the post-earthquake scenario: case studies in L'Aquila. Geomat Nat Hazards Risk 8:87–103. https://doi.org/10.1080/19475705.2016.1176605

Dong L, Shan J (2013) A comprehensive review of earthquake-induced building damage detection with remote sensing techniques. ISPRS J Photogramm Remote Sens 84:85–99. https://doi.org/10.1016/j.isprsjprs.2013.06.011

Erkal BG (2017) The prototype of a software application for laser and image-based surface damage detection. In: Proceedings of the 2nd world congress on civil, structural, and environmental engineering (CSEE'17), pp 1–7

Federal Emergency Management Agency (FEMA) (2016) Damage assessment operations manual-A guide to assessing damage and impact

Fernandez Galarreta J, Kerle N, Gerke M (2015) UAV-based urban structural damage assessment using object-based image analysis and semantic reasoning. Nat Hazards Earth Syst Sci 15:1087–1101. https://doi.org/10.5194/nhess-15-1087-2015

Gomez C, Purdie H (2016) UAV-based photogrammetry and geocomputing for hazards and disaster risk monitoring–A review. Geoenvironmental Disasters 3:23. https://doi.org/10.1186/s40677-016-0060-y

Grünthal G (1998) European Macroseismic Scale 1998. Chaiers du Centre Européen de Géodynamique et de Séismologie, Luxembourg

Guldur B, Hajjar J (2016) Automated classification of detected surface damage from point clouds with supervised learning. In: Proceedings of the 33rd ISARC. Auburn, AL, USA, pp 307–313

Guldur Erkal B, Hajjar JF (2017) Laser-based surface damage detection and quantification using predicted surface properties. Autom Constr 83:285–302. https://doi.org/10.1016/j.autcon.2017.08.004

Jafari B, Khaloo A, Lattanzi D (2017) Deformation tracking in 3D point clouds via statistical sampling of direct cloud-to-cloud distances. J Nondestruct Eval 36:65. https://doi.org/10.1007/s10921-017-0444-2

Kayen R, Collins BD, Bawden G, Pack RT (2006) Earthquake deformation analysis using terrestrial scanning Laser-LIDAR technology. In: 8th US national conference on earthquake engineering. San Francisco, California, USA

Kiratzi A (2018) The 12 June 2017 Mw 6.3 Lesvos Island (Aegean Sea) earthquake: slip model and directivity estimated with finite-fault inversion. Tectonophysics 724–725:1–10. https://doi.org/10.1016/j.tecto.2018.01.003

Mukupa W, Roberts GW, Hancock CM, Al-Manasir K (2016) A review of the use of terrestrial laser scanning application for change detection and deformation monitoring of structures. Surv Rev 49:99–116. https://doi.org/10.1080/00396265.2015.1133039

Nimodia C, Deshmukh HR (2012) Android operating system. Softw Eng 3:10–13

Olsen MJ, Chen Z, Hutchinson T, Kuester F (2013) Optical techniques for multiscale damage assessment. Geomat Nat Hazards Risk 4:49–70. https://doi.org/10.1080/19475705.2012.670668

Olsen MJ, Cheung KF, YamazakI Y, Butcher S, Garlock M, Yim S, McGarity S, Robertson I, Burgos L, Young YL (2012) Damage assessment of the 2010 Chile earthquake and tsunami using terrestrial laser scanning. Earthq Spectra 28:S179–S197. https://doi.org/10.1193/1.4000021

Olsen MJ, Kayen R (2012) Post-earthquake and tsunami 3D laser scanning forensic investigations. Forensic engineering 2012. American Society of Civil Engineers, Reston, VA, pp 477–486

Papadimitriou P, Kassaras I, Kaviris G, Tselentis G-A, Voulgaris N, Lekkas E, Chouliaras G, Evangelidis C, Pavlou K, Kapetanidis V, Karakonstantis A, Kazantzidou-Firtinidou D,

Fountoulakis I, Millas C, Spingos I, Aspiotis T, Moumoulidou A, Skourtsos E, Antoniou V, Andreadakis E, Mavroulis S, Kleanthi M (2018) The 12th June 2017 Mw = 6.3 Lesvos earthquake from detailed seismological observations. J Geodyn 115:23–42. https://doi.org/10.1016/j.jog.2018.01.009

Papakonstantinou A, Doukari M, Moustakas A, Chrisovalantis D, Chaidas K, Roussou O, Athanasis N, Topouzelis K, Soulakellis N (2018) UAS multi-camera rig for post-earthquake damage 3D geovisualization of Vrisa village. In: Themistocleous K, Hadjimitsis DG, Michaelides S, Ambrosia V, Papadavid G (eds) Sixth international conference on remote sensing and geoinformation of the environment (RSCy2018). SPIE, p 52

Pesci A, Teza G, Bonali E, Casula G, Boschi E (2013) A laser scanning-based method for fast estimation of seismic-induced building deformations. ISPRS J Photogramm Remote Sens 79:185–198. https://doi.org/10.1016/j.isprsjprs.2013.02.021

Puente I, Lindenbergh R, Van Natijne A, Esposito R, Schipper R (2018) Monitoring of progressive damage in buildings using laser scan data. In: ISPRS Int Arch Photogramm Remote Sens Spat Inf Sci XLII-2:923–929. https://doi.org/10.5194/isprs-archives-xlii-2-923-2018

Schütz M (2016) Potree: rendering large point clouds in web. Master Thesis, Vienna University of Technology

Snavely N (2011) Scene reconstruction and visualization from internet photo collections: a survey. IPSJ Trans Comput Vis Appl 3:44–66. https://doi.org/10.2197/ipsjtcva.3.44

Snavely N, Seitz SM, Szeliski R (2008) Modeling the world from internet photo collections. Int J Comput Vis 80:189–210. https://doi.org/10.1007/s11263-007-0107-3

Song M, Yousefianmoghadam S, Mohammadi M-E, Moaveni B, Stavridis A, Wood RL (2018) An application of finite element model updating for damage assessment of a two-story reinforced concrete building and comparison with lidar. Struct Heal Monit 17:1129–1150. https://doi.org/10.1177/1475921717737970

Triggs B, McLauchlan PF, Hartley RI, Fitzgibbon AW (2000) Bundle adjustment—a modern synthesis. In: Lecture Notes in Computer Science, pp 298–372

Westoby MJ, Brasington J, Glasser NF, Hambrey MJ, Reynolds JM (2012) 'Structure-from-Motion' photogrammetry: a low-cost, effective tool for geoscience applications. Geomorphology 179:300–314. https://doi.org/10.1016/j.geomorph.2012.08.021

Xu Z, Yang J, Peng C, Wu Y, Jiang X, Li R, Zheng Y, Gao Y, Liu S, Tian B (2014) Development of an UAS for post-earthquake disaster surveying and its application in Ms7.0 Lushan Earthquake, Sichuan, China. Comput Geosci 68:22–30. https://doi.org/10.1016/j.cageo.2014.04.001

Yamazaki F, Matsuda T, Denda S, Liu W (2015) Construction of 3D models of buildings damaged by earthquakes using UAV aerial images. In: Proceedings of the tenth pacific conference earthquake engineering building an earthquake-resilient pacific

Zhao X, Kargoll B, Omidalizarandi M, Xu X, Alkhatib H (2018) Model selection for parametric surfaces approximating 3D point clouds for deformation analysis. Remote Sens 10:634. https://doi.org/10.3390/rs10040634

Zhihua X, Lixin W, Yonglin S, Qiuling W, Ran W, Fashuai L (2014) Extraction of damaged building's geometric features from multi-source point clouds. In: 2014 IEEE geoscience and remote sensing symposium, IEEE, pp 4764–4767